Eur. Phys. J. B **57**, 27–35 (2007)
DOI: 10.1140/epjb/e2007-00148-9

THE EUROPEAN PHYSICAL JOURNAL B

Transport properties of a single-quantum dot Aharonov-Bohm interferometer

D.N. Son[1,a], N. Arboleda Jr[1], W.A. Dino[1,2,3], and H. Kasai[1,b]

[1] Department of Precision Science & Technology and Applied Physics, Graduate School of Engineering, Osaka University, Suita, Osaka 565-0871, Japan
[2] Department of Physics, Graduate School of Science, Osaka University, Toyonaka, Osaka 560-0043, Japan
[3] Center for the Promotion of Research in Nanoscience and Nanotechnology, Osaka University, Toyonaka, Osaka 560-0043, Japan

Received 12 January 2007 / Received in final form 12 April 2007
Published online 25 May 2007 – © EDP Sciences, Società Italiana di Fisica, Springer-Verlag 2007

Abstract. We consider a two-terminal Aharonov-Bohm (AB) interferometer with a quantum dot inserted in one path of the AB ring. We investigate the transport properties of this system in and out of the Kondo regime. We utilize perturbation theory to calculate the electron self-energy of the quantum dot with respect to the intradot Coulomb interaction. We show the expression of the Kondo temperature as a function of the AB phase together with its dependence on other characteristics such as the linewidth of the ring and the finite Coulomb interaction and the energy levels of the quantum dot. The current oscillates periodically as a function of the AB phase. The amplitude of the current oscillation decreases with increasing Coulomb interaction. For a given temperature, the electron transport through the AB interferometer can be selected to be in or out of the Kondo regime by changing the magnetic flux threading perpendicular to the AB ring of the system.

PACS. 73.63.-b Electronic transport in mesoscopic or nanoscale materials and structures – 73.21.La Quantum dots

1 Introduction

In typical systems of nanometer scale — such as a quantum ring and a quantum dot — the wave nature of electrons contributes a crucial role. In the Aharonov-Bohm (AB) interferometer [1–12], electron waves travel from the source to the drain along two different paths of the ring. The accumulated phase difference between these waves can be changed by applying a magnetic field. Experiments show that transport through the AB interferometer with a quantum dot inserted in one path of the ring has the following striking features: (i) the AB phase increases sharply by π; (ii) the transmission amplitudes at the various resonances are in phase; (iii) the transport is partially coherent in the presence of a strong intradot Coulomb interaction [1–8,10–12]; (iv) in the Kondo regime, the Kondo enhanced valley conductance is observed over a finite dc bias applied across the quantum dot [4,5,8]. Hackenbroich and Weidenmuller calculated the entire scattering amplitude through the AB interferometer and reported on the phase coherent transport through the quantum dot in the frame of the single particle scattering theory [13,14]. They focused on the AB phase and showed that as a function of the voltage on the dot, only the amplitude of the current oscillations is changed. The AB phase is unaffected unless this amplitude changes sign. In this case, the AB phase suddenly jumps by π. To consider several factors that may influence the system, Kim and Hershfield [15] studied the thermoelectric effects of this system when the quantum dot lies in the Kondo regime and when it is directly connected with two leads. Electrons can flow from one lead to the other through the two paths by direct tunneling (lead to lead) and a resonant tunneling via the quantum dot (lead to dot to lead). Interference between resonant transport through the quantum dot and the direct channel gives rise to asymmetric line shapes in the linear conductance as a function of the bias voltage (i.e. the well-known Fano effect) [9,16–18]. Bulka and Stefanski [19], and Hofstetter et al. [20] studied the combination of the Kondo effect and the Fano effect [21,22]. The electron transport through the quantum dot showed that the interference of the traveling waves with the localized state can lead to the Fano effect, for which the current characteristics are strongly modified in the Kondo regime. The source-drain voltage

[a] e-mail: son@dyn.ap.eng.osaka-u.ac.jp
[b] e-mail: kasai@dyn.ap.eng.osaka-u.ac.jp

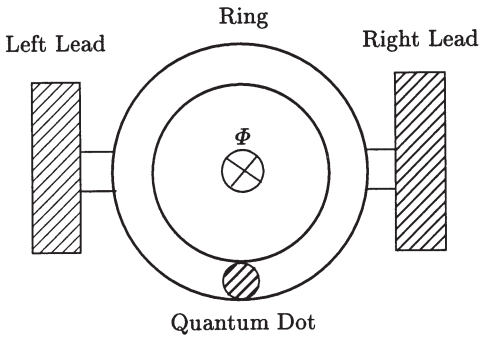

Fig. 1. A schematic description of the AB interferometer.

dependence exhibits a large peak or a dip, depending on the interference conditions.

How the intradot Coulomb interaction influences the phase coherence of electronic transport though the AB interferometer has been the subject of debate. Several theoretical papers concluded that the intradot Coulomb interaction induces partial dephasing from the spin-flip process [23–25], while others argued that the intradot Coulomb interaction does not induce dephasing effect at all and transport through the quantum dot is fully coherent [26]. These works have been devoted to investigate the properties of the AB interferometer in the small ring limit [23–26]. In this paper, we explore the transport properties of the system in the large ring limit [27,28].

As a first step to address this concern, We consider a two-terminal AB interferometer (see Fig. 1) with an AB ring and a quantum dot inserted in one of the ring's paths [1–5,7–10]. To investigate the electron transport through the system in or out of the Kondo regime, we consider a system with an indirect tunneling channel (lead to ring to lead) and a resonant tunneling channel via the dot (lead to ring to dot to ring to lead). In this AB interferometer, the quantum dot can be considered as an impurity [29] based on the Anderson model [30]. Hence, we can study the electron transport through the system as a function of the impurity characteristics and derive a reliable expression of the Green function for the quantum dot. To study the transport properties, we obtain the total current through the AB interferometer using the current formulation for interacting systems [31]. Here, the current is calculated using Green functions. The equation of motion method [32] is used to calculate the noninteracting Green functions. We then obtain the interacting Green functions using Dyson's equation where the perturbation method is utilized to calculate the self-energy of the quantum dot with respect to the intradot Coulomb interaction. This method can give high accuracy results [33].

We obtain the self-energy terms of the quantum dot in and out of the Kondo regime, expressed in terms of the AB phase and the universal functions involving the ratios of the temperature and the energy of the system to the Kondo temperature. Our results show that the coherent currents for different Coulomb interactions are in phase [1,2,13] and that the intradot Coulomb interaction can decrease the amplitude of the current oscillation. For a given temperature, the electron transport through the AB interferometer can be selected to be in or out of the Kondo regime by changing the magnetic flux threading perpendicular to the AB ring of the system. This is a new and interesting transport property of the AB interferometer.

The transport properties of the AB interferometer have been investigated also by Gerland et al. [34], Amasha et al. [35], and Fuhrer et al. [36] using the expression of the Kondo temperature of an impurity not in a magnetic field found in the works of Haldane [37], and Tsvelick and Wiegmann [38]. Recently, the Kondo temperature of the quantum dot in the AB interferometer has also been studied by Simon et al. [39], and Lewenkopf and Weidenmuller [40]. Simon et al. had shown the expression for the Kondo temperature as a function of the AB phase in the limit of infinite intradot Coulomb interaction in the tight binding Hamiltonian [39]. Lewenkopf and Weidenmuller utilized poor man's scaling and renormalization group arguments to investigate numerically the Kondo temperature of the quantum dot [40]. They discussed this temperature regime qualitatively in order to illustrate the action of the stochastic term in their model. The precise form of the dependence of the Kondo temperature on an AB phase cannot be predicted.

By using the method of canonical transformations introduced by Schrieffer and Wolff [41] and the renormalization group, we find a new explicit expression for the Kondo temperature as a function of the AB phase, together with its dependence on the finite intradot Coulomb interaction, the linewidth of the ring and the energy levels of the quantum dot.

2 Theory

2.1 Model Hamiltonian

We can express the Hamiltonian for the present system, with the quantum dot as an impurity, as follows

$$H = H_0 + H_{\rm T} + H_{\rm C}. \tag{1}$$

Here, H_0 describes the totally isolated subsystems of two leads, the AB ring, and the quantum dot, and is given by

$$H_0 = \sum_{k\sigma,\alpha={\rm L,R}} \epsilon_{k\alpha} c^{\alpha+}_{k\sigma} c^{\alpha}_{k\sigma} + \sum_{p\sigma} \epsilon_p c^{+}_{p\sigma} c_{p\sigma} + \sum_{\sigma} \epsilon_d d^{+}_{\sigma} d_{\sigma}, \tag{2}$$

where α stands for the left (L) and the right (R) leads, while k and $\epsilon_{k\alpha}$ are the longitudinal wave number and the corresponding energy of the electron. The energies of the single particle states within the ring and within the quantum dot are ϵ_p and ϵ_d, respectively. $c^{\alpha+}_{k\sigma}$, $c^{+}_{p\sigma}$, d^{+}_{σ} ($c^{\alpha}_{k\sigma}$, $c_{p\sigma}$, d_{σ}) are the creation (annihilation) operators for the electron in the leads, the ring, and the dot, respectively, while σ is the spin index. The tunneling part $H_{\rm T}$ consists

of the couplings between the subsystems, and is given by

$$H_{\rm T} = \sum_{kp\sigma,\alpha={\rm L,R}} (W^{\alpha}_{kp\sigma} c^{\alpha+}_{k\sigma} c_{p\sigma} + h.c) + \sum_{p\sigma} \left[\left(V^{\rm l}_{pd} + V^{\rm r}_{pd} e^{-i\phi} \right) c^{+}_{p\sigma} d_{\sigma} + h.c \right], \quad (3)$$

where the tunneling matrix elements $W^{\alpha}_{kp\sigma}$ describe the coupling between the ring and the leads, while the tunneling matrix elements $V^{\rm l}_{pd}$ ($V^{\rm r}_{pd}$) describe the coupling between the left (right) side of the dot and the ring. According to the AB effect, when electron waves from two paths of the ring meet again, the phase difference between the electron waves will be an AB phase factor $\exp(-i\phi)$, where $\phi = 2\pi\Phi e/h$ and Φ is the magnetic flux enclosed by the ring formed by the paths. We attach the magnetic flux on the right hand side of the dot, hence, $V^{\rm r}_{pd}$ carries an AB phase factor $\exp(-i\phi)$. The intradot Coulomb interaction Hamiltonian is given by,

$$H_{\rm C} = U n_{\uparrow} n_{\downarrow}, \quad (4)$$

where U is the charging energy of the quantum dot. n_{σ} is the number operator, $n_{\sigma} = d^{+}_{\sigma} d_{\sigma}$.

2.2 The Kondo temperature of the quantum dot in the Aharonov-Bohm interferometer

In the present work, we are concerned with an AB interferometer in the large ring limit. We can assume that the dimension of the ring is much greater than the size of the Kondo screening cloud. Hence, electrons in the leads play a minor role, or $W^{\alpha}_{kp\sigma} < V^{\rm l,r}_{pd}$. This assumption will be used throughout the paper. Thus, the following part of the Hamiltonian (1) can be utilized to define a coupling constant J between the quantum dot and the rest of the system, that is,

$$\bar{H} = \sum_{p\sigma} \epsilon_p c^{+}_{p\sigma} c_{p\sigma} + \sum_{\sigma} \epsilon_d d^{+}_{\sigma} d_{\sigma} + U n_{\uparrow} n_{\downarrow} + \sum_{p\sigma} \left[(V^{\rm l}_{pd} + V^{\rm r}_{pd} e^{-i\phi}) c^{+}_{p\sigma} d_{\sigma} + h.c \right]. \quad (5)$$

By means of Schrieffer-Wolff transformation [41], the Anderson Hamiltonian (5) can be mapped onto the Kondo Hamiltonian in the form

$$\bar{H} = \sum_{p\sigma} \epsilon_p c^{+}_{p\sigma} c_{p\sigma} + \sum_{p\alpha,p'\beta} J_{p,p'} c^{+}_{p\alpha} \boldsymbol{\sigma} c_{p'\beta} . \boldsymbol{S_d}, \quad (6)$$

where $\boldsymbol{S_d} = d^{+}_{\sigma} (\boldsymbol{\sigma_{\alpha\beta}}) d_{\beta}$. The Pauli matrices and the spin of the localized moment of the quantum dot are denoted by $\boldsymbol{\sigma}$ and $\boldsymbol{S_d}$, respectively. This Hamiltonian describes the localized moment that is coupled to the conduction electron band by the exchange interaction $J_{p,p'}$,

$$J_{p,p'} = \left(V^{\rm l}_{pd} + V^{\rm r}_{pd} e^{-i\phi} \right) \left(V^{\rm l*}_{p'd} + V^{\rm r*}_{p'd} e^{i\phi} \right) \times \left(\frac{1}{\epsilon_p - \epsilon_d} + \frac{1}{\epsilon_d + U - \epsilon_{p'}} \right). \quad (7)$$

For ϵ_p and $\epsilon_{p'}$ near the Fermi level ϵ_F and for $\epsilon_d < \epsilon_F < \epsilon_d + U$, the exchange interaction $J_{p,p'}$ is approximately

$$J = -2|V_d|^2 (1 + \cos\phi) \frac{U}{\epsilon_d (\epsilon_d + U)}. \quad (8)$$

Here, the tunneling matrix elements $V^{\rm l}_{pd}$ ($V^{\rm r}_{pd}$) are assumed to be real and equal to V_d. The antiferromagnetic constant is J. To show the relationship between J and the Kondo temperature, we must utilize the renormalization group.

The renormalization group enables us to write the renormalization flow equation up to the third order of the running coupling constant $J\rho$ for $\cos\phi \neq -1$ as follows,

$$\frac{\partial (J\rho)}{\partial \ln D} = -2(J\rho)^2 + 2(J\rho)^3 + O\left((J\rho)^4\right). \quad (9)$$

Here, D is the cutoff energy or the energy of the largest excitations while ρ is the density of states of the ring. Integrating this equation for $D' \ll D$, we obtain

$$\ln\left(\frac{D'}{D}\right) = -\frac{1}{2J\rho} + \frac{1}{2}\ln(2J\rho) + O(1). \quad (10)$$

The Kondo temperature T_K, where the system scales to strong coupling (very large $J\rho$), is obtained by setting $D' = T_K$ in the equation (10), which gives

$$T_K = D\sqrt{2J\rho} \exp\left(-\frac{1}{2J\rho}\right). \quad (11)$$

Equation (11) expresses the relationship between T_K and J. From (8) and (11), we can deduce the Kondo temperature of the quantum dot for the cutoff energy U as

$$T_K = U\sqrt{-\frac{2\Delta(1+\cos\phi)U}{\pi\epsilon_d(\epsilon_d+U)}} \exp\left(\frac{\pi\epsilon_d(\epsilon_d+U)}{2\Delta(1+\cos\phi)U}\right). \quad (12)$$

Here, $\Delta = 2\pi\rho|V_d|^2$ is the linewidth of the ring and ϕ is the AB phase. This expression shows the dependence of the Kondo temperature of the quantum dot on the AB phase (see also Fig. 3), which does not appear in the works of Haldane [37] and Tsvelick and Wiegmann [38]. Also, the linewidth Δ of the ring appears instead of the leads' [37,38].

For $\cos\phi \longrightarrow -1$, we have $T_K \longrightarrow 0$ K.

2.3 The total current through the Aharonov-Bohm interferometer

The current through the system from the leads to the central region (the ring-dot) is calculated from the time evolution of the occupation numbers in the leads, $N_{\alpha} = \sum_k c^{\alpha+}_{k\sigma} c^{\alpha}_{k\sigma} (\alpha = {\rm L,R})$, by (see Ref. [31])

$$I_{\alpha}(t) = -\frac{ie}{h} \langle [H, N_{\alpha}] \rangle. \quad (13)$$

By using equations (1–4) for (13), one finds

$$I_{\alpha}(t) = \frac{ie}{h} \sum_{kp\sigma} \left[W^{\alpha}_{kp\sigma} \left\langle c^{\alpha+}_{k\sigma} c_{p\sigma} \right\rangle - W^{\alpha*}_{kp\sigma} \left\langle c^{+}_{p\sigma} c^{\alpha}_{k\sigma} \right\rangle \right]. \quad (14)$$

Applying the Keldysh Green function technique found in the work of Jauho et al. [31], we define two Green functions

$$G^{<}_{p\sigma,k\sigma\alpha}(t,t') = i\langle c^{\alpha+}_{k\sigma}(t')c_{p\sigma}(t)\rangle, \quad (15)$$

$$G^{<}_{k\sigma\alpha,p\sigma}(t,t') = i\langle c^{+}_{p\sigma}(t')c^{\alpha}_{k\sigma}(t)\rangle. \quad (16)$$

Using $G^{<}_{k\sigma\alpha,p\sigma}(t,t) = -\left[G^{<}_{p\sigma,k\sigma\alpha}(t,t)\right]^{*}$ and the model of noninteracting leads [31], after integrating over time t' from $-\infty$ to t , we have

$$I_\alpha = \frac{ie}{h}\sum_{p\sigma\sigma'}\int\frac{d\epsilon}{2\pi}\left\{\Gamma^{\alpha}(\epsilon)\left(G^{<}_{p\sigma\sigma'}(\epsilon) + f_\alpha(\epsilon)\right.\right. \times[G^{r}_{p\sigma\sigma'}(\epsilon) - G^{a}_{p\sigma\sigma'}(\epsilon)]\left.\left.\right)\right\}. \quad (17)$$

Here, the linewidth of the leads is $\Gamma^{\alpha}(\epsilon) = 2\pi\sum_k W^{\alpha*}_{kp\sigma} W^{\alpha}_{kp\sigma}\delta(\epsilon-\epsilon_{k\alpha})$, $\alpha = (\mathrm{L},\mathrm{R})$. The Fermi distribution function of the leads is $f_{\mathrm{L(R)}}(\epsilon)$. The energy of incoming electrons is ϵ. The retarded and advanced Green functions of the ring-dot are $G^{r,a}_{p\sigma\sigma'}(\epsilon)$.

In the steady state, the current is uniform such that $I = I_{\mathrm{L}} = I_{\mathrm{R}}$. We can symmetrize the current by $I = (I_{\mathrm{L}} - I_{\mathrm{R}})/2$. Using equation (17) and the assumption that the left and right linewidth functions $\Gamma^{\mathrm{L,R}}(\epsilon)$ are proportional to each other, the proportional parameter can be chosen so that the Green function $G^{<}_{p\sigma\sigma'}(\epsilon)$ vanishes (see Ref. [31]), and we have

$$I = \frac{ie}{h}\sum_{p\sigma\sigma'}\int\frac{d\epsilon}{2\pi}\frac{\Gamma^{\mathrm{L}}(\epsilon)\Gamma^{\mathrm{R}}(\epsilon)}{\Gamma^{\mathrm{L}}(\epsilon)+\Gamma^{\mathrm{R}}(\epsilon)} \times\left\{\left[f_{\mathrm{L}}(\epsilon) - f_{\mathrm{R}}(\epsilon)\right]\left[G^{r}_{p\sigma\sigma'}(\epsilon) - G^{a}_{p\sigma\sigma'}(\epsilon)\right]\right\}. \quad (18)$$

Equation (18) gives us the total current for the system. The calculation of the Green functions requires the consideration of Coulomb interaction in the quantum dot.

To calculate the retarded and advanced Green functions $G^{r,a}_{p\sigma\sigma'}(\epsilon)$ of the ring-dot, we first calculate the retarded and advanced noninteracting Green functions $G^{(r,a)0}_{p\sigma\sigma'}(\epsilon)$ of the ring-dot and $G^{(r,a)0}_{\sigma\sigma'}(\epsilon)$ of the dot using the equation of motion method. We then calculate the retarded and advanced interacting Green functions of the dot $G^{r,a}_{\sigma\sigma'}(\epsilon)$ using Dyson's equation. These steps are detailed as follows.

Using the equation of motion method yields equations (19–21) which give the relationship among the noninteracting Green functions of the quantum dot $G^{(r,a)0}_{\sigma\sigma'}(\epsilon)$, the ring-dot $G^{(r,a)0}_{p\sigma\sigma'}(\epsilon)$, and the dot-leads $G^{(r,a)\alpha0}_{k\sigma\sigma'}(\epsilon)$ (the index 0 denotes the noninteracting Green function);

$$(\epsilon-\epsilon_d\pm i\delta)G^{(r,a)0}_{\sigma\sigma'}(\epsilon) = 1 + \sum_{p'}(V^{\mathrm{l}*}_{p'd} + V^{\mathrm{r}*}_{p'd}e^{i\phi}) \times G^{(r,a)0}_{p'\sigma\sigma'}(\epsilon), \quad (19)$$

$$(\epsilon-\epsilon_p\pm i\delta)G^{(r,a)0}_{p\sigma\sigma'}(\epsilon) = \sum_{k\alpha} W^{\alpha*}_{kp\sigma}G^{(r,a)\alpha0}_{k\sigma\sigma'}(\epsilon) + (V^{\mathrm{l}}_{pd} + V^{\mathrm{r}}_{pd}e^{-i\phi})G^{(r,a)0}_{\sigma\sigma'}(\epsilon), \quad (20)$$

$$(\epsilon-\epsilon_{k\alpha}\pm i\delta)G^{(r,a)\alpha0}_{k\sigma\sigma'}(\epsilon) = \sum_{p'} W^{\alpha}_{kp'\sigma}G^{(r,a)0}_{p'\sigma\sigma'}(\epsilon). \quad (21)$$

Here, δ is an infinitesimal quantity. All matrix elements W and V do not change appreciably on the scale of charging energy. We can assume that W and V are independent of k and p. Solving the set of equations (19–21) for $G^{(r,a)0}_{p\sigma\sigma'}(\epsilon)$ and $G^{(r,a)0}_{\sigma\sigma'}(\epsilon)$ with $V^{\mathrm{l}}_{pd} = V^{\mathrm{r}}_{pd} = V^{\mathrm{l}*}_{pd} = V^{\mathrm{r}*}_{pd} = V_d$, we have

$$G^{(r,a)0}_{p\sigma\sigma'}(\epsilon) = \frac{V_d(1+e^{-i\phi})}{\epsilon-\epsilon_p\pm i\delta}G^{(r,a)0}_{\sigma\sigma'}(\epsilon), \quad (22)$$

and

$$G^{(r,a)0}_{\sigma\sigma'}(\epsilon) = \frac{1}{\epsilon-\epsilon_d\pm i\Delta(1+\cos\phi)}. \quad (23)$$

For the interacting Green functions, equation (22) can be generalized in the following form

$$G^{r,a}_{p\sigma\sigma'}(\epsilon) = \frac{V_d(1+e^{-i\phi})}{\epsilon-\epsilon_p\pm i\delta}G^{r,a}_{\sigma\sigma'}(\epsilon). \quad (24)$$

Using Dyson's equation

$$G^{r,a}_{\sigma\sigma'}(\epsilon) = \frac{G^{(r,a)0}_{\sigma\sigma'}(\epsilon)}{1-\Sigma^{r,a}(\epsilon)G^{(r,a)0}_{\sigma\sigma'}(\epsilon)}, \quad (25)$$

and substituting (23) to (25), we obtain the interacting Green functions for the quantum dot

$$G^{r,a}_{\sigma\sigma'}(\epsilon) = \frac{1}{\epsilon-\epsilon_d\pm i\Delta(1+\cos\phi)-\Sigma^{r,a}(\epsilon)}. \quad (26)$$

Here $\Sigma^{r,a}$ are the retarded and advanced self-energy terms, which can be calculated using the method found in the work of Yoshimori and Kasai [42] for two different energy and finite temperature regimes of the system.

2.3.1 Current in the Kondo regime

In this regime, the energy ϵ and the temperature T of the system are much smaller than the Kondo temperature $\epsilon < T_K$, and $T < T_K$. Provided that the Kondo temperature is far smaller than the cutoff energy, $T_K \ll D$, the low energy governs the physics of the Kondo effect. For this reason, we expect all physical quantities to be expressed in terms of universal functions involving the ratios of the temperature and the energy of the system to the Kondo temperature (i.e., T/T_K, ϵ/T_K).

For $\cos\phi \neq -1$, the self-energy (see Appendix) is determined by

$$\Sigma^{r,a}(\epsilon) = \Delta(1+\cos\phi)\left\{\frac{\epsilon}{T_K} \pm \frac{i}{2}\left[\left(\frac{\epsilon}{T_K}\right)^2 + \left(\frac{\pi T}{T_K}\right)^2\right]\right\}, \quad (27)$$

where T is the finite temperature of the system, T_K is the Kondo temperature defined by (12), and Δ is the linewidth of the ring. The self-energy depends indirectly

on the Coulomb interaction through the Kondo temperature.

Using equations (27, 26, 24) and (18), we get

$$I = \frac{e}{h}\frac{\Gamma^{\mathrm{L}}\Gamma^{\mathrm{R}}}{\Gamma^{\mathrm{L}}+\Gamma^{\mathrm{R}}}\sum_p \frac{[f_{\mathrm{L}}(\epsilon_p) - f_{\mathrm{R}}(\epsilon_p)]\,(1+\cos\phi)A}{[A^2 + \Delta^2(1+\cos\phi)^2(1+B)^2]}, \quad (28)$$

where A and B are

$$A = [\epsilon_p - \epsilon_d + \Delta(1+\cos\phi)\epsilon_p/T_K]\,, \quad (29)$$

and

$$B = \frac{1}{2}\left[\left(\frac{\epsilon}{T_K}\right)^2 + \left(\frac{\pi T}{T_K}\right)^2\right], \quad (30)$$

respectively, and $\Gamma^{\alpha}(\alpha = \mathrm{L},\mathrm{R}) < \Delta < U$, due to $W^{\alpha} < V_d$ and the cut off energy is equal to U.

2.3.2 Current out of the Kondo regime

In this regime, the temperature T of the system is higher than the Kondo temperature $T > T_K$. For $\cos\phi \neq -1$ and $U > \Delta$, the self-energy at the Fermi level is determined by

$$\Sigma^{r,a} \approx i\Delta(1+\cos\phi)\frac{\ln(T/T_K) + \sqrt{\ln^2(T/T_K) + 3\pi^2/4}}{\ln(T/T_K) - \sqrt{\ln^2(T/T_K) + 3\pi^2/4}}, \quad (31)$$

where T is the finite temperature of the system, T_K is the Kondo temperature defined by (12), Δ is the linewidth of the ring.

Using equations (31, 26, 24) and (18), we get

$$I = \frac{e}{h}\frac{\Gamma^{\mathrm{L}}\Gamma^{\mathrm{R}}}{\Gamma^{\mathrm{L}}+\Gamma^{\mathrm{R}}}\sum_p \frac{[f_{\mathrm{L}}(\epsilon_p) - f_{\mathrm{R}}(\epsilon_p)]\,(1+\cos\phi)\,(\epsilon_p - \epsilon_d)}{(\epsilon_p-\epsilon_d)^2 + \Delta^2(1+\cos\phi)^2(1-C)^2}, \quad (32)$$

where

$$C = \frac{\ln(T/T_K) + \sqrt{\ln^2(T/T_K) + 3\pi^2/4}}{\ln(T/T_K) - \sqrt{\ln^2(T/T_K) + 3\pi^2/4}}, \quad (33)$$

and $\Gamma^{\alpha}(\alpha = \mathrm{L},\mathrm{R}) < \Delta < U$, since $W^{\alpha} < V_d$ and the cut off energy is equal to U.

For $\cos\phi = -1$, $I = 0$ A.

3 Results and discussion

To simulate our results, we introduce a symmetric model with $\epsilon_d = -U/2$. The energy diagram of the dot and its density of states (i.e., the dotted line) are described in Figure 2. Resonant tunneling between the two leads occurs and current flows when an energy level in the dot is aligned with the Fermi level in the ring and in the leads. When one of the dot levels drops below the Fermi level in the ring, this level becomes occupied and the number of electrons increases by one in the dot. In order to scan the levels in the dot over the Fermi level, a plunger gate can be used [1–12]. By changing the plunger gate voltage, one can change ϵ_d, U, as well as the number of electrons in the quantum dot. Chemical potentials μ_{L} and μ_{R} in the left and right leads are e V and 0 V, respectively, for all situations of the transport which are demonstrated in this paper.

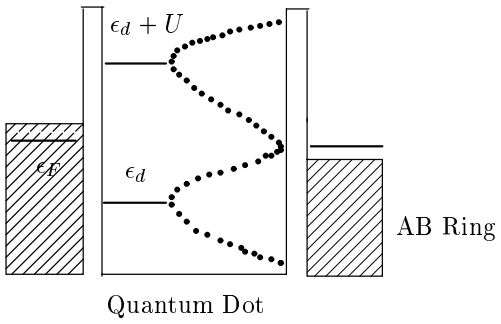

Fig. 2. The energy diagram of the quantum dot and its density of states (i.e., the dotted line). U and ϵ_d are the Coulomb interaction and the energy level of the quantum dot, respectively. ϵ_F is the Fermi level of the ring. At low temperature, there will be a sharp peak at the Fermi level (the Kondo peak).

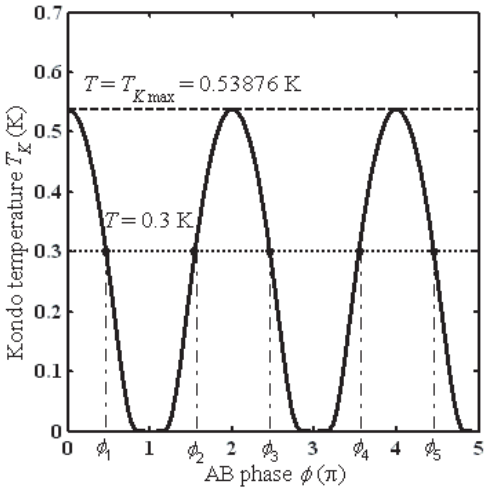

Fig. 3. The dependence of the Kondo temperature T_K on the AB phase for $U = 1$ V and $\Delta = U/2$.

Figure 3 shows the Kondo temperature dependence on the AB phase (the solid line), for $U = 1$ V and $\Delta = U/2$ (this value of the linewidth ensures smaller than the cut-off energy U of the Kondo temperature). When the quantum dot is isolated from the system by setting V_d to 0 V or the AB phase value to an odd multiple of π, the Kondo temperature approaches zero asymptotically. When the quantum dot is connected to the system or the AB phase is not an odd multiple of π, the spin exchange between the dot and the ring exists, and the Kondo temperature has maxima at an even multiple of π. We also determined numerically the Kondo temperature for several other values

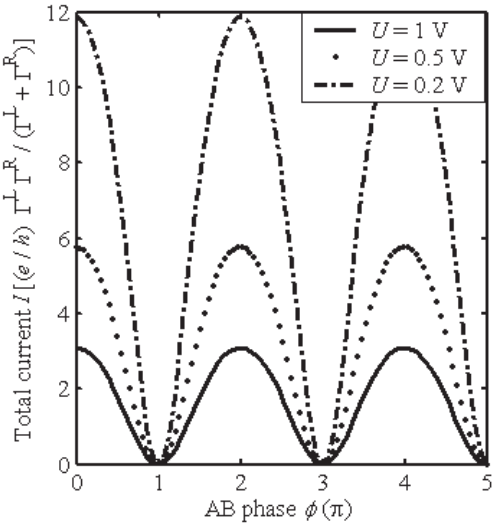

Fig. 4. The dependence of the total current I on the AB phase in the Kondo regime for $T = 0$ K; $\epsilon_p = 0$ V; $U = 1$ V, 0.5 V, and 0.2 V; $\Delta = U/10$; and $\Gamma^\alpha(\alpha = \mathrm{L}, \mathrm{R}) < \Delta < U$.

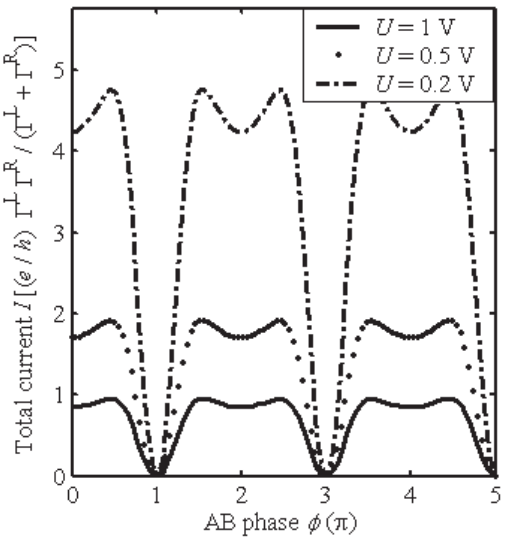

Fig. 5. The dependence of the total current I on the AB phase in the Kondo regime for $T = 0$ K; $\epsilon_p = 0$ V; $U = 1$ V, 0.5 V, and 0.2 V; $\Delta = U/2$; and $\Gamma^\alpha(\alpha = \mathrm{L}, \mathrm{R}) < \Delta < U$.

of the Coulomb interaction U (not shown here). We arrive at a conclusion that the Kondo temperature of the quantum dot, although dependent on the AB phase, is always less than 1 K.

The electron transport through the AB interferometer can be in or out of the Kondo regime depending on the value of its temperature. Figure 3 shows that the possible temperature T of the interferometer can be in one of three regions: lower than the minimum of T_K ($T = 0$ K), from the minimum to the maximum of T_K ($0 < T < T_{K\max} = 0.53876$ K), and equal to or higher than the maximum of T_K ($T \geq T_{K\max}$).

For $T = 0$ K (T less than the minimum of T_K), the system definitely works in the Kondo regime. The transport through the system obeys the expression (28) and is governed by the cotunneling process, which involves the simultaneous tunneling of two or more electrons (the Kondo effect). The dependence of the total current I on the AB phase in this situation is depicted in Figures 4 and 5 for $\epsilon_p = 0$ V (compared to the Fermi level), and for three different values of U (i.e., 0.2 V, 0.5 V, and 1 V), with linewidths of the ring of $U/10$ and $U/2$, respectively. Here (as well as in Figs. 6 and 7), we chose the current when the quantum dot is disconnected from the ring as the reference current, hence, the total current also corresponds to the coherent current. Figure 4 shows that, when the linewidth of the ring is small or when the coupling between the quantum dot and the ring is weak, the total current has constructive interference around an even multiple of π. Away from the constructive interference, the current quickly vanishes. Figure 5 shows that, when the linewidth of the ring is large or when the coupling between the quantum dot and the ring is strong, the constructive interference in Figure 4 is now split into two peaks.

For $0 < T < T_{K\max}$, the Kondo temperature is changed when the AB phase (i.e., the magnetic flux) is changed. This means that the electron transport through the system is alternatively in or out of the Kondo regime for the fixed temperature T when the magnetic flux is changed. The electron transport obeys either (28) or (32). The total current in this context is depicted in Figure 6 for the fixed temperature $T = 0.3$ K and ϵ_p is from 0 V to $0.1 k_B T_K$ (k_B is the Boltzmann constant), as an example. The line $T = 0.3$ K (the dotted line in Fig. 3) intersects the line T_K at points ϕ_1, ϕ_2, ϕ_3, ϕ_4, and ϕ_5 (see Fig. 3). For the AB phase in ranges: $[0, \phi_1]$, $[\phi_2, \phi_3]$ and $[\phi_4, \phi_5]$, $T_K > T$ and the transport through the interferometer is in the Kondo regime and governed by the cotunneling process. The current is described by the solid lines in Figure 6. For the AB phase in ranges: $[\phi_1, \phi_2]$, $[\phi_3, \phi_4]$ and $[\phi_5, 5\pi]$, $T_K < T$ and the transport is out of the Kondo regime and governed by the sequential tunneling process. The current is described by the dotted lines in Figure 6. From these results, we can conclude that the transport through the system at a given temperature can be selected to be in or out of the Kondo regime by controlling the magnetic flux. This is a new result which can give experimentalists new and interesting topics.

For $T \geq T_{K\max}$, the transport is certainly out of the Kondo regime, hence, expression (32) is used. The current as a function of the AB phase is described in Figure 7 for $T = 2$ K (T higher than maximum of T_K); ϵ_p is from 0 V to $0.1 k_B T_{K\max}$ (k_B is the Boltzmann constant) , and for three different values of U (i.e., 0.2 V, 0.5 V, and 1 V), with $\Delta = U/2$. Even though the linewidth is large, the peaks of the total current cannot be split. Since, in this regime the contribution from the conduction electron spin moment to the transport of the whole system is negligible. The transport process is sequential tunneling. An increase

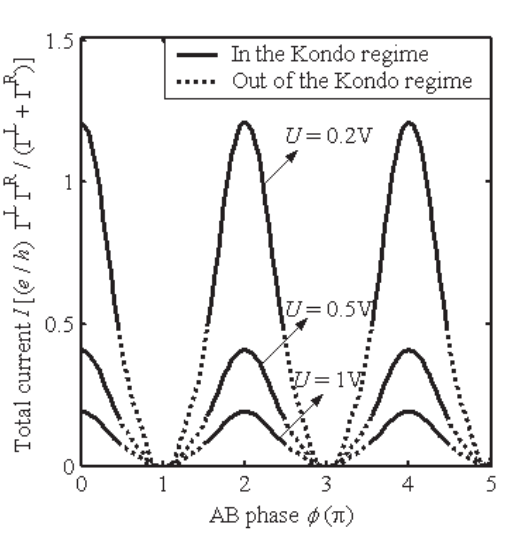

Fig. 6. The dependence of the total current I on the AB phase in the Kondo regime (solid lines) and out of the Kondo regime (dotted lines) for $T = 0.3$ K; $\epsilon_p \in [0, 0.1k_BT_K]$ V ; $U = 1$ V, 0.5 V, and 0.2 V; $\Delta = U/2$; and $\Gamma^\alpha(\alpha = \mathrm{L}, \mathrm{R}) < \Delta < U$.

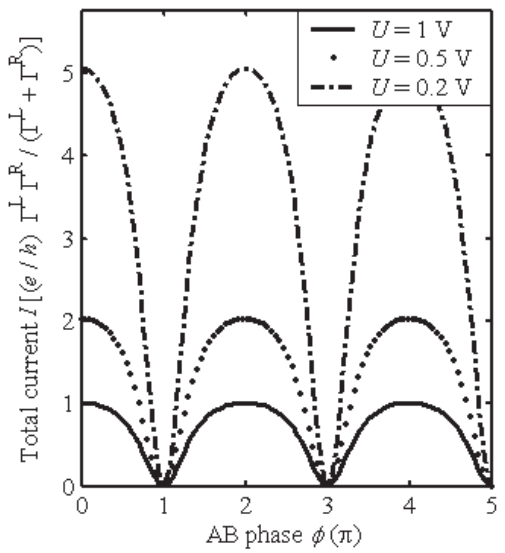

Fig. 7. The dependence of the total current I on the AB phase out of the Kondo regime for $T = 2$ K; $\epsilon_p \in [0, 0.1k_BT_{K\max}]$ V; $U = 1$ V, 0.5 V, and 0.2 V; $\Delta = U/2$; and $\Gamma^\alpha(\alpha = \mathrm{L}, \mathrm{R}) < \Delta < U$.

of the linewidth of the ring only widens the peaks of the total current.

Figures 4–7 show that as U increases, the amplitude of the oscillations of the total current decreases. If we take a look at equation (3), we find that the coupling between the quantum dot and the ring, i.e., $V_{pd}^{\mathrm{l}} + V_{pd}^{\mathrm{r}} \exp(-i\phi)$ and $V_{pd}^{\mathrm{l}*} + V_{pd}^{\mathrm{r}*} \exp(i\phi)$ with $V_{pd}^{\mathrm{l}} = V_{pd}^{\mathrm{r}} = V_{pd}^{\mathrm{l}*} = V_{pd}^{\mathrm{r}*}$, becomes zero when ϕ equals an odd multiple of π. Hence, the part of the Hamiltonian which describes the tunneling between the quantum dot and the ring disappears from equation (3). This means that the quantum dot is isolated from the system. Thus, the total current for any arbitrary U reaches a minimum value, i.e., the total current is not affected by the intradot Coulomb interaction when the AB phase is an odd multiple of π. The figures also show that the AB oscillations are all in phase.

The quantum dot can be isolated from or connected with the ring by controlling the AB phase forward or away from an odd multiple of π. We can also deduce that the Kondo temperature of the isolated quantum dot is zero.

Figures 4–7 also showed that the current oscillations for different values of U are in phase. The transport is coherent in the presence of Coulomb interaction. These results are in a good agreement with experiments.

The single-electron transmission through an AB ring with electron-electron interactions has been studied by Zitko and Bonca [24]. The integrated transmission probability is presented as a function of the magnetic flux for different values of electron-electron interactions within the ring. They showed that the amplitude of AB oscillations decreases with increasing electron-electron interaction. This is qualitatively agreeable to our result.

The exact linear conductance at zero temperature was calculated by Hofstetter et al using Keldysh formalism, the Friedel sum rule, and numerical renormalization group [20]. They showed that the conductance as a function of the AB phase reaches its maximum at $\phi = \pi/2$. This dependence is similar to a function of $\sin\phi$. This agrees with the result of Konig and Gefen [25] for the AB interferometer with the small ring limit. Making comparisons to the work of Konig and Gefen [25], our self-energy terms depend on the AB phase of $(1 + \cos\phi)$ and the linewidth Δ of the ring, while those of Konig and Gefen depend on $\sin\phi$ and the linewidth of the leads. Konig and Gefen considered the small ring limit in their system. Results for the AB interferometer at the large ring limit may be derived from those for the small ring limit by changing $(1 + \cos\phi)$ with $\sin\phi$ and vice versa. These imply that the different limits of the ring's size cause different dependences of the transport properties on the system's parameters.

4 Conclusion

We found a new expression for the Kondo temperature of the quantum dot in the two-terminal AB interferometer as a function of the AB phase (i.e., the magnetic flux), the finite intradot Coulomb interaction, the linewidth of the ring, and the energy levels of the quantum dot. We also obtained new self-energy terms of the quantum dot and the current expression of the system in and out of the Kondo regime, which were expressed in terms of the AB phase and universal functions involving the ratios of the temperature and the energy of the system to the Kondo temperature. The amplitude of the current oscillation decreases with increasing intradot Coulomb interaction. For a given temperature, the electron transport through the AB interferometer can be selected to be in or out of the Kondo regime by changing the magnetic flux threading

perpendicular to the AB ring of the system. The Kondo temperature of the isolated quantum dot is zero.

This work was partially supported by the 21st Century COE program (G18) from the Japan Society for the Promotion of Science (JSPS), and a Grant-in-Aid for Scientific Research on Priority Areas (Developing Next Generation Quantum Simulators and Quantum-Based Design Techniques) by the Ministry of Education, Culture, Sports, Science and Technology (MEXT).

Appendix A

The Fourier component of the perturbed Green function is expanded in a power series of U as

$$G(\epsilon_n) = G^0(\epsilon_n) - \sum_{n=1}^{\infty} \frac{U^{2n}}{(2n)!}\frac{1}{\beta}\int_0^\beta ... \int_0^\beta e^{i\epsilon_n(t-t')} dt dt' dt_1 ...dt_{2n} \left[\sum_{ji} G^0_{ti} G^0_{jt'} [D^{2n}(1,2,...,2n)]^2\right]_{\text{connected}}, \quad \text{(A.1)}$$

where

$$G^0_{ij} = \frac{1}{\beta}\sum_n G^0(\epsilon_n) e^{-i\epsilon_n(t_i - t_j)}, \quad \text{(A.2)}$$

$$G^0(\epsilon_n) = \frac{1}{i(\epsilon_n + \Delta(1+\cos\phi)\text{sgn}\epsilon_n)}, \quad \text{(A.3)}$$

$$\epsilon_n = \frac{1}{\beta}(2n+1), \quad \text{(A.4)}$$

and $\beta = 1/k_B T$ (k_B is the Boltzmann constant).

Noting the relation

$$G(\epsilon_n) = G^0(\epsilon_n) + G^0(\epsilon_n)\Sigma(\epsilon_n)G^0(\epsilon_n). \quad \text{(A.5)}$$

From (A.1) and (A.5), the self energy is defined by

$$\Sigma(\epsilon_n) = -\sum_{n=1}^{\infty} \frac{U^{2n}}{(2n)!}\frac{1}{\beta} \times \int_0^\beta ... \int_0^\beta dt_1 ...dt_{2n} \left[\sum_{ji} e^{-i\epsilon_n(t_j - t_i)} [D^{2n}]^2\right]_{\text{connected}}, \quad \text{(A.6)}$$

where D^{2n} is defined through G^0_{ij} by the following $2n$th order determinant

$$D^{2n} = \begin{vmatrix} 0 & G^0_{12} & G^0_{13} & ... & G^0_{1(2n)} \\ G^0_{21} & & & & \vdots \\ \vdots & & & & \vdots \\ G^0_{(2n)1} & ... & ... & ... & 0 \end{vmatrix}. \quad \text{(A.7)}$$

At low temperature and low energy region, the self energy can be expanded as a function of $U/[\Delta(1+\cos\phi)]$ for $\cos\phi \neq -1$ and $\Delta \neq 0$, as follows

$$\Sigma^{r,a}(\epsilon_n) = \Delta(1+\cos\phi)\left\{0.5\left[\frac{U}{\Delta(1+\cos\phi)}\right]^2 + 0.05\left[\frac{U}{\Delta(1+\cos\phi)}\right]^4 + ...\right\}\frac{\epsilon_n}{\Delta(1+\cos\phi)} \pm \frac{i\Delta(1+\cos\phi)}{2} \times \left\{\left[\frac{U}{\Delta(1+\cos\phi)}\right]^2 + 2.5\left[\frac{U}{\Delta(1+\cos\phi)}\right]^4 + ..\right\} \times \left\{\left[\frac{\epsilon_n}{\Delta(1+\cos\phi)}\right]^2 + \left[\frac{\pi T}{\Delta(1+\cos\phi)}\right]^2\right\} + ... \quad \text{(A.8)}$$

or

$$\Sigma^{r,a}(\epsilon) \approx \Delta(1+\cos\phi)\left\{\frac{\epsilon}{T_K} \pm \frac{i}{2}\left[\left(\frac{\epsilon}{T_K}\right)^2 + \left(\frac{\pi T}{T_K}\right)^2\right]\right\}. \quad \text{(A.9)}$$

References

1. A. Yacoby, M. Heiblum, D. Mahalu, H. Shtrikman, Phys. Rev. Lett. **74**, 4047 (1995)
2. R. Schuster, E. Buks, M. Heiblum, D. Mahalu, V. Umansky, H. Shtrikman, Nature (London) **385**, 417 (1997)
3. E. Buks, R. Schuster, M. Heiblum, D. Mahalu, V. Umansky, Nature (London) **391**, 871 (1998)
4. Y. Ji, M. Heiblum, D. Sprinzak, D. Mahalu, H. Shtrikman, Science **290**, 779 (2000)
5. Y. Ji, M. Heiblum, H. Shtrikman, Phys. Rev. Lett. **88**, 076601 (2002)
6. A.W. Holleitner, C.R. Decker, H. Qin, K. Eberl, R.H. Blick, Phys. Rev. Lett. **87**, 256802 (2001)
7. H. Aikawa, K. Kobayashi, A. Sano, S. Katsumoto, Y. Iye, Phys. Rev. Lett. **92**, 176802 (2004)
8. W.G. van der Wiel, S. De Franceschi, T. Fujisawa, J.M. Elzerman, S. Tarucha, L.P. Kouwenhoven, Science **289**, 2105 (2000)
9. K. Kobayashi, H. Aikawa, S. Katsumoto, Y. Iye, Phys. Rev. Lett. **88**, 256806 (2002)
10. M. Avinun-Kalish, M. Heiblum, O. Zarchin, D. Mahalu, V. Umansky, Nature (London) **436**, 529 (2005)
11. M. Sigrist, A. Fuhrer, T. Ihn, K. Ensslin, S.E. Ulloa, W. Wegscheider, M. Bichler, Phys. Rev. Lett. **93**, 066802 (2004)
12. M. Sigrist, T. Ihn, K. Ensslin, D. Loss, M. Reinwald, W. Wegscheider, Phys. Rev. Lett. **96**, 036804 (2006)
13. G. Hackenbroich, Phys. Rep. **343**, 463 (2001)
14. G. Hackenbroich, H.A. Weidenmuller, Phys. Rev. Lett. **76**, 110 (1996)
15. T.-S. Kim, S. Hershfield, Phys. Rev. B **67**, 165313 (2003)
16. U. Fano, Phys. Rev. **124**, 1866 (1961)
17. K. Kobayashi, H. Aikawa, S. Katsumoto, Y. Iye, Phys. Rev. B **68**, 235304 (2003)
18. T. Nakanishi, K. Terakura, T. Ando, Phys. Rev. B **69**, 115307 (2004)
19. B.R. Bulka, P. Stefanski, Phys. Rev. Lett. **86**, 5128 (2001)

20. W. Hofstetter, J. Konig, H. Schoeller, Phys. Rev. Lett. **87**, 156803 (2001)
21. T. Kawasaka, H. Kasai, W.A. Dino, A. Okiji, J. Appl. Phys. **86**, 6970 (1999)
22. W.A. Dino, K. Imoto, H. Kasai, A. Okiji, Jpn J. Appl. Phys. **39**, 4359 (2000)
23. H. Akera, Jpn J. Appl. Phys. **38**, 384 (1999)
24. R. Zitko, J. Bonca, Phys. Rev. B **68**, 085313 (2003)
25. J. Konig, Y. Gefen, Phys. Rev. B **65**, 045316 (2002)
26. Z.-T. Jiang, Q.-F. Sun, X.C. Xie, Y. Wang, Phys. Rev. Lett. **93**, 076802 (2004); Z.-T. Jiang, Q.-F. Sun, X.C. Xie, Y. Wang, Phys. Rev. Lett. **94**, 179702 (2005)
27. P. Simon, I. Affleck, Phys. Rev. Lett. **89**, 206602 (2002)
28. P. Simon, I. Affleck, Phys. Rev. B **68**, 115304 (2003)
29. J. von Delft, Science **289**, 2064 (2000)
30. P.W. Anderson, Phys. Rev. **124**, 41 (1961)
31. A.P. Jauho, N.S. Wingreen, Y. Meir, Phys. Rev. B **50**, 5528 (1994)
32. J. Fransson, Phys. Rev. B **72**, 075314 (2005)
33. V. Kashcheyevs, A. Aharony, O. Entin-Wohlman, Phys. Rev. B **73**, 125338 (2006)
34. U. Gerland, J. von Delft, T.A. Costi, Y. Oreg, Phys. Rev. Lett. **84**, 3710 (2000)
35. S. Amasha, I.J. Gelfand, M.A. Kastner, A. Kogan, Phys. Rev. B **72**, 045308 (2005)
36. A. Fuhrer, T. Ihn, K. Ensslin, W. Wegscheider, M. Bichler, Phys. Rev. Lett. **93**, 176803 (2004)
37. F.D.M. Haldane, Phys. Rev. Lett. **40**, 416 (1978)
38. A.M. Tsvelick, P.B. Wiegmann, Adv. Phys. **32**, 453 (1983)
39. P. Simon, O. Entin-Wohlman, A. Aharony, Phys. Rev. B **72**, 245313 (2005)
40. C.H. Lewenkopf, H.A. Weidenmuller, Phys. Rev. B **71**, 121309(R) (2005)
41. J.R. Schrieffer, P.A. Wolff, Phys. Rev. **149**, 491 (1966)
42. A. Yoshimori, H. Kasai, Solid State Communications **58**, 259 (1986)